

ORIGINAL ARTICLE

Altered Expression of Reorganized Inputs as They Ascend From the Cuneate Nucleus to Cortical Area 3b in Monkeys With Long-Term Spinal Cord Injuries

Priyabrata Halder, Niranjana Kambi, Prem Chand and Neeraj Jain

National Brain Research Centre, N.H. 8, Manesar, Haryana 122051, India

Address correspondence to Neeraj Jain, National Brain Research Centre, N.H. 8, Manesar, Haryana 122051, India.

Email: neeraj.jain@nbrc.ac.in; njain.nbrc@gmail.com

Abstract

Chronic deafferentations in adult mammals result in reorganization of the brain. Lesions of the dorsal columns of the spinal cord at cervical levels in monkeys result in expansion of the intact chin inputs into the deafferented hand representation in area 3b, second somatosensory (S2) and parietal ventral (PV) areas of the somatosensory cortex, ventroposterior lateral nucleus (VPL) of the thalamus, and cuneate nucleus of the brainstem. Here, we describe the extent and nature of reorganization of the cuneate and gracile nuclei of adult macaque monkeys with chronic unilateral lesions of the dorsal columns, and compare it with the reorganization of area 3b in the same monkeys. In both, area 3b and the cuneate nucleus chin inputs expand to reactivate the deafferented neurons. However, unlike area 3b, neurons in the cuneate nucleus also acquire receptive fields on the shoulder, neck, and occiput. A comparison with the previously published results shows that reorganization in the cuneate nucleus is similar to that in VPL. Thus, the emergent topography following deafferentations by spinal cord injuries undergoes transformation as the reorganized inputs ascend from subcortical nuclei to area 3b. The results help us understand mechanisms of the brain plasticity following spinal cord injuries.

Key words: dorsal columns, *Macaca*, nucleus gracilis, somatosensory, ventroposterior nucleus

Receptive field properties of neurons undergo transformation as tactile inputs ascend from the brainstem nuclei to ventroposterior nucleus of the thalamus and then to cortical somatosensory areas. Response properties of neurons in the network are determined by the extent of convergence and divergence of the feedforward inputs, intrinsic connections, including modulation by inhibitory interneurons and feedback influence from the upstream areas (Lee et al. 1994b; Dykes and Craig 1998; Ergenzinger et al. 1998; Krupa et al. 1999; Temereanca and Simons 2004; Wilson et al. 2012; Liao et al. 2013). Deafferentations due to peripheral nerve, spinal cord or brain injuries alter the network balance by sprouting, degeneration and readjustment of the synaptic strengths induced by changes in the input patterns (Ralston et al. 1996; Ergenzinger et al. 1998; Florence et al. 1998; Jones and Pons 1998; Pluto et al. 2004; Graziano and Jones 2009). Plasticity in multiple regions of the brain has been

shown following acute and chronic injuries in many different mammalian species including rats, cats, flying foxes, many different species of monkeys and humans (Dostrovsky et al. 1976; Merzenich et al. 1983; Calford and Tweedale 1988; Turnbull and Rasmusson 1991; Jain et al. 1997; Grüsser et al. 2004; Tandon et al. 2009; see Kaas et al. 2008; Jain and Tandon 2012 for review). While the plasticity following acute injuries is likely due to unmasking of previously silent inputs, the exact mechanisms of plasticity following chronic injuries remain poorly understood.

Injuries that cause large deafferentations, such as lesions of the dorsal columns of the spinal cord or transection of the dorsal roots from C2 to T1 result in large-scale topographic reorganization at multiple levels in the brain. Following these injuries most of the neurons in the deafferented hand representation in the primary somatosensory cortex, that is, area 3b, get reactivated

by intact chin inputs (Pons et al. 1991; Jain et al. 1997, 2008; Liao et al. 2016b). Similar expansion of the face representation also takes place in the somatosensory cortex of humans with spinal cord injuries (e.g., Brown-Séquard syndrome or tetraplegia; Corbetta et al. 2002; Saadon-Grosman et al. 2015). Reorganization is also seen in the second somatosensory (S2) and the parietal ventral (PV) areas, ventroposterior lateral nucleus (VPL) of the thalamus, and cuneate nucleus of the brainstem (Jain et al. 2008; Tandon et al. 2009; Kambi et al. 2014).

Reorganization at multiple levels of the somatosensory network is also observed following a more limited deafferentation due to transection of sensory nerves to the hand or digit amputations. Following such injuries reactivation of the deafferented neurons, which is limited to inputs from the same body part, is observed in areas 3b and 1 of the cortex, VPL of the thalamus and cuneate nucleus of the brainstem (Merzenich et al. 1983, 1984; Xu and Wall 1997, 1999a; Churchill et al. 2001).

However, network properties of the somatosensory pathway influence the expression of emergent receptive fields at each level following reorganization. For example, reorganization in a small region of the brain can influence neuronal responses in large parts of the network. A recent report from our laboratory showed that following partial spinal cord injuries, expression of chin inputs in the deafferented parts of area 3b is a result of expression of these inputs in the cuneate nucleus (Kambi et al. 2014), which is likely due to axonal sprouting (Jain et al. 2000). We have also shown that expression of the face inputs in the hand region of area 3b takes place following recovery periods of 6 months or more after lesions of the dorsal columns (Jain et al., 1997), further suggesting sprouting as one of the possible mechanisms for brain plasticity. Previous reports of large-scale reorganization have focused on expansion of the face input into the deafferented regions of the brain (Pons et al. 1991; Jain et al. 1997, 2008). Here we determined the nature of emergent receptive fields at different levels along the somatosensory neuraxis—the brainstem nuclei and area 3b. We first provide a detailed description of topography in the reorganized cuneate and gracile nuclei following chronic unilateral lesions of dorsal columns of the spinal cord at cervical levels in adult macaque monkeys. These details are not available at present. We then compare the nature of receptive fields in the cuneate nucleus with that in area 3b of the same monkeys. Finally, we compare and discuss these data with the published descriptions of reorganization in VPL.

Materials and Methods

All animal procedures were approved by the Institutional Animal Ethics Committee (IAEC) of National Brain Research Centre, and

the Committee for the Purpose of Control and Supervision of Experiment in Animals (CPCSEA), Government of India.

Animals

Cuneate nucleus and area 3b were mapped in 4 adult macaque monkeys with long-term lesions of the dorsal columns (two male *Macaca radiata*, and 2 male *Macaca mulatta*, weighing between 7.7 and 11.3 kg at the time of the lesion; Table 1). The brain was mapped after more than 14 months of recovery period. In addition, normal organization of the cuneate nucleus was determined in 2 monkeys without any lesions (*Macaca mulatta*, 1 female and 1 male, weighing 4.3 and 10.5 kg, respectively; Table 1). Some of these animals were also used in previously reported studies (Kambi et al. 2014; Chand and Jain 2015).

Lesions of the Dorsal Columns

Procedures for dorsal column lesions have been described before (Tandon et al. 2009). Briefly, the animals were anesthetized using a mixture of ketamine (8 mg/kg, IM) and xylazine (0.4 mg/kg, IM). Supplemental doses of the anesthetics were given at one-tenth of the initial dose as required during the course of surgery. Animals were given dexamethasone (2 mg/kg, IM) and glycopyrrolate (0.015 mg/kg IM) before starting the surgery. The neck and upper back were prepared and a midline incision was made in the skin. The muscles were retracted to expose the vertebrae, a partial laminectomy was done, dura was incised and the dorsal columns on the left side were transected unilaterally between C4 and C6 levels from midline to the point of entry of the dorsal roots using a pair of sharp fine forceps. While making the lesion care was taken to minimize damage to the surface blood vessels. The dura was folded back in place, the spinal cord was covered with a piece of absorbable sponge (AbGel, Mumbai, India), the muscles and the skin were sutured in layers and the animals were allowed to recover from anesthesia under constant monitoring. Heart rate, blood oxygenation levels, and core body temperature were continuously monitored during the entire procedure. The animals were given antibiotics, analgesics, and dexamethasone for 5 days postsurgery (Tandon et al. 2009). The animals were carefully monitored for food and fluid intake. No complications were observed and the recoveries were uneventful.

Multiunit Mapping of Area 3b

Somatotopy of area 3b contralateral to the lesion was determined using standard multiunit electrophysiological techniques as described before (Jain et al. 2008; Tandon et al. 2009).

Table 1 Details of the monkeys and number of recording sites

Animal	Macaca species	Sex	Weight (kg)	Recovery period (months)	Weight (kg)	Number of recording sites (includes nonresponsive sites)	
						Cortex	Cuneate nucleus
06-39NM	Rhesus	Female	4.3	–	4.3	627	285
06-65NM	Rhesus	Male	10.5	–	10.5	372	86
LM76*	Rhesus	Male	9.3	20	9.3	260	284
10-50LM*	Bonnet	Male	7.7	16	7.7	361	170
LM49*	Bonnet	Male	7.7	14	7.7	391	122
LM59*	Rhesus	Male	11.3	43	11.3	360	326

*Monkeys with dorsal columns lesions.

Briefly, the animals were anesthetized with ketamine (8 mg/kg, IM) and xylazine (0.4 mg/kg, IM), and the head of the animal was fixed in a stereotaxic head holder (Kopf, Tujunga, CA, USA). Anesthesia was maintained by additional doses of ketamine and xylazine as required, and supplemented with urethane (250 mg/kg IP, every 8 h). The depth of anesthesia was monitored and maintained by checking the eyelid and toe-pinch reflex, as well as by continuously monitoring the heart rate. Dexamethasone (2 mg/kg, IM) was administered to prevent swelling of the brain. Blood oxygenation levels were continuously monitored during the entire procedure. Core body temperature was monitored with a rectal probe and maintained at 37°C with a warm-water blanket placed under the monkey. Additional heat was provided by an infrared lamp, if required. Saline was administered intravenously, alternating with dextrose (5% in saline) every 4 h. The monkeys were given enrofloxacin (5 mg/kg; IM) and glycopyrrolate (0.015 mg/kg; IM) every 24 h during these long mapping sessions.

A midline incision was made in the skin of the head, and the muscles were retracted. A craniotomy was made over area 3b to expose the brain. The dura was incised and reflected, and the brain was covered with warm silicone to prevent desiccation. A photograph of the brain surface was taken and printed at a large magnification on which locations of the electrode penetration sites were marked.

Receptive fields of the neurons were determined at 300–400 μm intervals using a parylene coated tungsten microelectrode (1 MΩ at 1 kHz, Microprobe, MD, USA), which was advanced down the posterior bank of the central sulcus (Fig. 1A) using a hydraulic Microdrive (Model 2650, David Kopf Instruments, CA, USA). At each recording site, the entire body was thoroughly explored for neuronal responses to light tactile stimulation, taps, and movements of the joints and muscles. Our efforts were mainly focused on stimulating receptive fields on the contralateral half of the body. The responses were qualitatively classified based on the kind of stimulus required into those requiring light touch, hair stimulation, taps, hard taps, or movements of joints. Receptive fields were carefully drawn on photographs of the body surface of each monkey. The electrode penetrations were spaced to cover the entire hand and face regions of area 3b. We made a total of 81 penetrations in the 4 lesioned monkeys and recorded from 1372 sites (see Table 1 for details). In the 2 normal monkeys we made 43 penetrations and recorded from 999 sites (Table 1). Our main goal here was to qualitatively characterize neuronal responses over the largest possible expanse of area 3b. However, in a few animals for a different set of experiments limited quantitative data was collected at some of the recording sites using a computer controlled tactile stimulator, which is illustrated in Kambi et al. (2014).

Multinuit Mapping of the Brainstem Nuclei

Brainstem nuclei were mapped in the same session as area 3b. The entire mapping session lasted from 2 to 4 days. For mapping the brainstem nuclei, the animals were kept anesthetized using the same regimen of anesthetics and other drugs as described above for area 3b. The head of the animal was stabilized in a stereotaxic frame, and the frame was tilted to ventrally flex the neck. A midline incision was made over the medulla, and the neck muscles were retracted. A few millimeters of the occipital bone overlying the cerebellum was carefully removed using a pair of sharp rongeurs. The ventral-most part of the vermis of the cerebellum was removed by subpial aspiration using a low vacuum for better access to medulla. The dura over

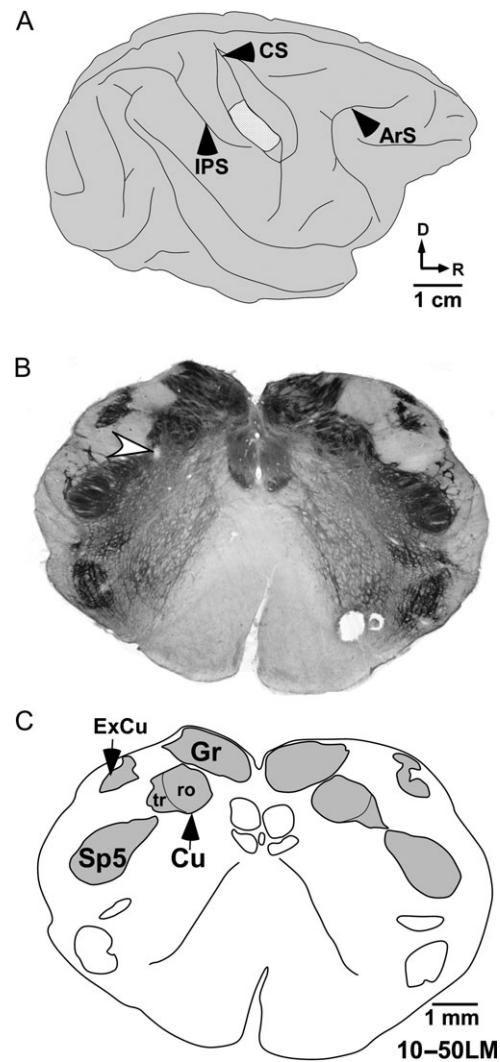


Figure 1. (A) An outline diagram of the dorsolateral view of a macaque monkey brain. The central sulcus (CS) is shown opened to illustrate the approximate region of area 3b that was mapped (light grey). Intraparietal sulcus (IPS) and the arcuate sulcus (ArS) are labeled for reference. D, dorsal; R, rostral. (B) Photomicrograph of a coronal section through the medulla of macaque monkey 10-50LM. The section was stained for cytochrome oxidase activity to reveal nuclear boundaries. The cuneate, gracilis, and spinal trigeminal nuclei are clearly visible (c.f. "C"). The white arrowhead points to a focal lesion made to help align the electrode track with the electrophysiological map (see [Materials and Methods](#)). (C) Outline diagram of the section shown in "B" with the cuneate (Cu), gracile (Gr), spinal trigeminal (Sp5) and external cuneate (ExCu) nuclei marked. Pars rotunda (ro) and pars triangularis (tr) of the cuneate nucleus are also marked. Scale bar also applies to "B".

the fourth ventricle was reflected to expose the brainstem. For mapping, a tungsten microelectrode was positioned approximately perpendicular to the dorsal surface of the medulla. The electrode was advanced using the hydraulic microdrive and receptive fields of neurons were determined every 100 or 200 μm along the dorsoventral axis. The receptive fields, primarily focusing on the ipsilateral side of the body were determined as described above for area 3b. Since the goal was to sample maximal extent of the nuclei in the available time, we first made rows of spaced penetrations to determine boundaries of the nuclei and to sample the neuronal response properties. Subsequently additional penetrations were made to

increase the density of the recording sites. Recordings started 100 μm below the dorsal surface of the medulla and continued until no responses were encountered at 2–3 successive depths. We recorded from 902 sites by making 125 penetrations in the ipsilateral medulla of the 4 monkeys with lesions (Table 1). In the 2 normal monkeys the receptive fields were determined at 371 recording sites by making 36 penetrations (Table 1). Receptive fields and neuronal responses were noted as described above for area 3b. In addition to the cuneate nucleus, recordings were made from the gracile nucleus and parts of the spinal trigeminal nucleus (Fig. 1B, C). The quantitative data collected at some of the recording sites for a different set of experiments is shown in Kambi et al. (2014).

At the end of the mapping experiments the animals were deeply anesthetized with a high dose of Pentothal (17.5 mg/kg), and perfused transcardially sequentially with phosphate buffered saline (0.1 M, pH 7.4), buffered 3% or 4% paraformaldehyde, and paraformaldehyde containing 10% sucrose (Tandon et al. 2009). The monkey LM59 was perfused with 2% fixatives because we flattened the cortex of this animal (Jain et al., 1998).

Identification of Locations and Orientations of the Electrode Tracks

We used 3 different methods to help identify orientations and locations of the electrode tracks in area 3b and the brainstem nuclei. One, some of the tracks were marked by passing a cathodal current of 10 μA as the electrode was withdrawn at the rate of 25 $\mu\text{m}/\text{s}$, which left a track of burnt tissue. Two, we made focal lesions at selected recording sites at different depths by passing a current of 10 μA for 10 s (Fig. 1B). Finally, in monkey LM49 we also marked a few tracks by coating the electrode with DiI fluorescent dye prior to insertion (Kambi et al., 2014).

Histology

After perfusion, the brain was removed, the cortex separated from the subcortical tissue and cryoprotected in 30% sucrose. Cortex surrounding the central sulcus was blocked, frozen and cut into 60 μm thick sections on a sliding microtome in a plane perpendicular to the central sulcus, which is slightly off the parasagittal plane. A series of sections from the cortex were stained for cytochrome oxidase (CO) activity. Other series of sections were stained for Nissl substance and acetylcholinesterase (AChE) activity to visualize the areal and laminar boundaries (Kambi et al. 2011). For the lesioned monkey LM59 the cortex was flattened and cut in a plane tangential to the pial surface in 40 μm thick sections. One series of sections was stained for myelin and the other 2 were used to visualize neuroanatomical tracers injected for unrelated studies (Chand and Jain 2015).

Medulla was cut in a coronal plane into 36, 40, or 50 μm thick sections depending upon the number of series of sections required for different treatments. One series of sections was stained for CO activity to visualize boundaries of the nuclei, the other series was mounted unstained to visualize fluorescent electrode tracks (Kambi et al. 2014), or processed for neuroanatomical tracers injected for unrelated studies.

Spinal cords of the lesioned monkeys were also removed, cryoprotected as above, and cut into 40 or 50 μm thick sections in a horizontal plane. The sections were mounted unstained and observed under dark-field illumination for reconstruction of the lesion site. For some monkeys a series of sections was processed to visualize neuroanatomical tracers injected for unrelated studies.

Reconstruction of the Somatosensory Map in Area 3b

The somatotopic map was reconstructed using Canvas X software (ACDSee, WA, USA) as described in detail before (Tandon et al. 2009). Neuronal responses requiring light touch, hair stimulation, taps or hard taps were represented by different symbols and marked accordingly. All the reconstructed tracks were assembled in their relative positions, and outlines of the different body part representations coded by different colors were drawn accordingly to visualize somatotopy in the posterior bank of the central sulcus.

Reconstruction of Somatotopic Map in the Cuneate Nucleus

The progression of receptive fields along the electrode tracks was first reconstructed as described for area 3b. These reconstructions were transferred to outline drawings of the sections of the medulla from the appropriate rostro-caudal level. The alignment was done with the help of the electrolytic lesions (Fig. 1B) and fluorescently marked electrode tracks.

Reconstruction of the Spinal Cord Lesion

Drawings of the spinal cord sections in the region of the lesion were made using a microscope equipped with camera lucida under dark-field illumination (Tandon et al. 2009). Maximal extent of the lesion, and boundaries of the white matter and grey matter were measured for each section, and plotted on a graph paper. The corresponding boundaries were joined to visualize extent of the lesion in a coronal plane (Fig. 2).

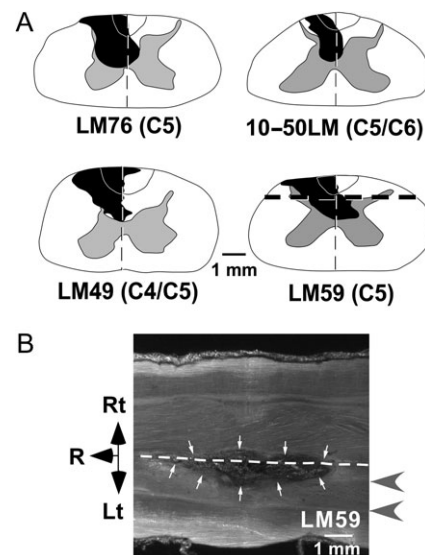


Figure 2. (A) Reconstruction of the spinal cords in a coronal plane showing extent of the lesions (black filled area). The monkey numbers and the level of the lesions are shown below each figure. The grey matter (filled with grey) and the midline (dashed vertical line) are shown. Boundary between the cuneate and gracile fasciculus is also drawn. On the lesioned side this boundary is mirror image from the opposite side for reference. The horizontal dashed line for LM59 marks the approximate location from where the section shown in “B” was taken. The spinal cord reconstructions for monkeys LM76, LM49, and LM59 have been published before (Kambi et al. 2014), and are shown here for ready reference. (B) Dark-field photomicrograph of a horizontal section of the spinal cord of monkey LM59 in the region of the lesion (surrounded by white arrows). Grey arrowheads on the right mark the medial and lateral boundaries of the grey matter, and the dashed line marks the midline. R, rostral; Rt, right; Lt, left.

Statistics

If the dorsal column lesion was incomplete, hand responsive recording sites were observed in both the cuneate nucleus and area 3b. We determined if there is any correlation between the number of hand responsive recording sites in the cuneate nucleus and area 3b of monkeys. We first calculated the number of hand responsive sites as a percentage of total responsive sites in the cuneate nucleus and the hand region of area 3b and plotted as a scatter plot. Pearson's correlation coefficient and coefficient of determination was calculated and its statistical significance was determined using Student's *t*-test.

Results

We first briefly describe somatotopy in the normal cuneate and gracile nuclei, followed by reorganized somatotopy in these nuclei and area 3b in monkeys with spinal cord injuries. Finally, we compare topographic organization in the cuneate nucleus and area 3b of monkeys with lesions. No differences were obvious in results from the 2 species of macaque monkeys used, therefore, these results are considered together.

Normal Organization of the Cuneate and Gracile Nuclei

Somatotopic organization of the brainstem nuclei, particularly the cuneate nucleus has been described before in different monkey species (Florence et al. 1989; Xu and Wall 1996, 1999b; Strata et al. 2003; Darian-Smith and Ciferri 2006). Our results from the 2 normal monkeys, 06-39NM (Fig. 3) and 06-65NM (not shown) were similar. Here we briefly describe our results emphasizing only those features that are relevant for comparison with the lesioned monkeys.

In the cuneate nucleus digits and palm representations were located in the pars rotunda (Fig. 3B, D; also see Fig. 1B, C). Receptive fields on the digits progressed from proximal to distal in a dorsal to ventral direction in the nucleus. Representations of the digits were rotated in a manner such that the digit tips were more medial as compared with the proximal parts. This resulted in progression of receptive fields from ulnar to radial digits in dorsoventral penetrations in the medial parts of the nucleus (Fig. 3D, Penetration, abbreviated as Pen subsequently, #117). Neurons responded robustly to light touch on the hand. The receptive fields on the glabrous hand were small, encompassing only a small region of the glabrous digits (Fig. 3D). At a few locations receptive fields were on the dorsal skin of the hand (e.g., see Pen #120, Fig. 3D).

The arm representation was located lateral as well as dorsal to the hand representation. The lateral arm representation often extended through the dorsoventral extent of the nucleus. The receptive fields usually encompassed a part of the forearm or the upper arm. Sometimes a clear progression from proximal to distal arm in the dorsal to ventral direction was obvious (Fig. 3D, Pen #119). We did not find any arm representation in the medial part of the cuneate nucleus, although it has been found at this location in marmosets and squirrel monkeys (Xu and Wall 1996, 1999b) and proposed to be present in macaque monkeys (Florence et al. 1989).

Responses to touch on the occiput, neck, and upper shoulder were present in the lateral-most part of the cuneate nucleus, largely in the pars triangularis. We did not find these body part representations in the medial part of the cuneate nucleus. Previous results also show a lack of these representations in the medial part of the nucleus in squirrel monkeys and macaque monkeys (Edney and Porter 1986; Xu and Wall 1999b),

although it is present at this location in marmosets (Xu and Wall 1996). The receptive fields usually covered a small region of skin on these body parts (Fig. 3D, Pen #107, 112).

Through the gracile nucleus we recorded neuronal responses from 112 sites in 14 penetrations. Neurons responded to touch on the foot, leg, trunk, and tail (Fig. 3C, E; Qi and Kaas 2006). The receptive fields covered a small region on the skin of the foot or toes (Fig. 3E) with neurons responding to light touch or gentle brushing of hairs. We also observed a lateral to medial progression of receptive fields on the foot in the dorsoventral direction in a penetration (Fig. 3E, Pen #114).

We did not map the spinal trigeminal nucleus in detail. At the medial-most locations, adjacent to the cuneate nucleus, neurons responded to touch on the chin (not shown). Neurons responding to touch on the lips and other parts of the face were found at more lateral and ventral locations. Somatotopy in the spinal trigeminal nucleus was similar to that described before (Kerr et al. 1968; Jain et al. 2000; Liao et al. 2016a).

Organization of the Cuneate Nucleus in Monkeys With Dorsal Column Lesions

We determined somatotopy of the cuneate nucleus in 4 monkeys with chronic lesions of the dorsal columns. The maximal cross-sectional extent of the spinal cord lesions and their levels are shown in Figure 2.

At a large number of recording sites in the cuneate nucleus neurons responded to touch on the ipsilateral chin (75.3% of the responsive sites, $n = 396$; Figs 4 and 5; also see Fig. 8A; please note that for calculation of proportion of the sites responding to touch on a particular body part, the sites where neurons responded to more than one body part have been counted multiple times, once for each body part, resulting in a total of more than 100%). Neurons responding to chin stimulation were found in the entire dorsoventral and mediolateral extent of the nucleus (Figs 4B and 5B). At most of the locations neurons responded to taps rather than light touch. In normal animals neurons in the cuneate nucleus do not have receptive fields on the chin.

Throughout the pars rotunda of the cuneate nucleus in 3 monkeys (LM76, LM49, and LM59), where hand representation is normally expected, neurons also responded to touch on the occiput, neck, or upper shoulder (31.6% of the sites, $n = 396$; e.g., Fig. 4B, C, Pen #29 and 30; also see Fig. 8B). The neuronal responses were generally robust to the stimulation of the hairs, although at many sites receptive fields required taps for evoking a response (see, e.g., Fig. 4B, Pen #30, 53, and 54). However, these representations were not found in the pars rotunda of monkey 10-50LM, the monkey with the largest sparing of the hand inputs, except at one lateral-most location (Fig. 5B, Pen #20).

An expansion of the arm representation was also observed to a varying extent in different monkeys. There was ventralward expansion of the arm representation, which is normally confined to the dorsal-most region (Figs 4B and 5B; also see Fig. 8B). We also observed arm responsive sites in the medial part of the cuneate nucleus, which were not present in normal monkeys. The receptive fields were of similar size as in the normal monkeys, although occasionally they could be much larger covering an entire arm, shoulder and neck, or the arm and shoulder (Fig. 4, Pen #36 and 37). The responses were weaker and often required taps instead of stimulation of the hair.

We also found many recording sites in the cuneate nucleus where neurons responded to touch on the hand depending upon the extent of sparing of the dorsal column fibers. In monkey 10-50LM neurons at a large number of recording sites had responses

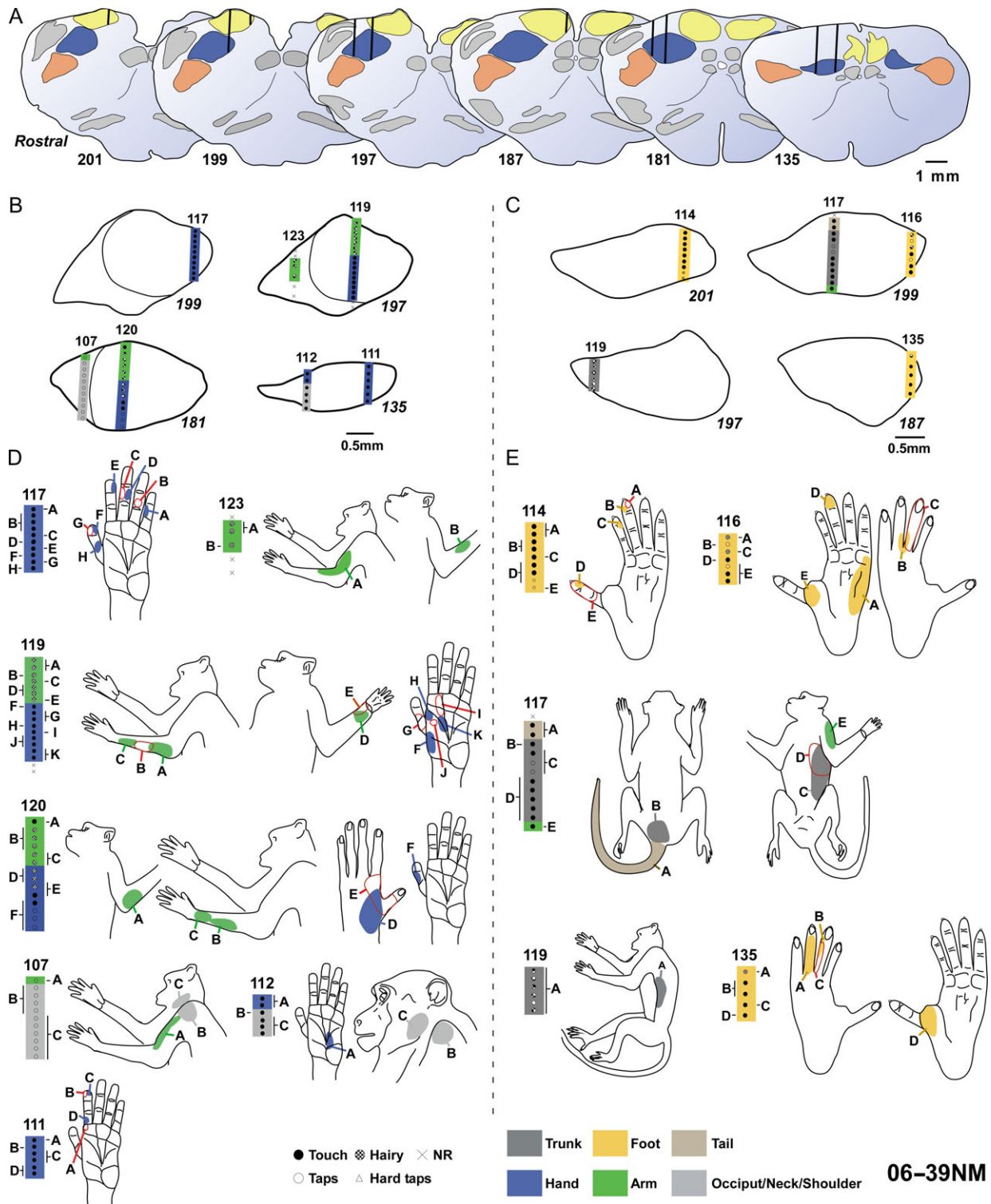


Figure 3. Organization of the normal cuneate and gracile nuclei of monkey 06-39NM. (A) Outline drawings of a series of sections through the medulla showing cuneate (blue), gracile (yellow) and spinal trigeminal (orange) nuclei. Black vertical lines show locations of the representative electrode penetrations shown in “B–E”. Rostral-most section is to the left. Section numbers are marked for reference. (B, C) Enlarged outline diagrams of the cuneate (B) and gracile (C) nucleus showing electrode tracks with location of the receptive fields on the body at the recording sites. Dots mark the recording sites where receptive fields were mapped. Different types of dots show the nature of the stimulus required to elicit a response (see key at the bottom). Sizes of the dots indicate strength of the response. Smaller dots indicate weaker responses. Locations of the receptive fields on the body are color coded as per the key at the bottom. Section numbers corresponding to those in “A” are labeled in italics. (D) Receptive fields of neurons at the recording sites in the cuneate nucleus for each penetration shown in “B”. Corresponding electrode penetration numbers in “B” and “C” are labeled with numbers on top. For each recording site corresponding receptive field(s) are marked with the same upper case letter on the adjacent figures of the monkey. The display is arranged to show the penetrations in the same sequence as in “B”. (E) Receptive fields of neurons in the nucleus gracilis along the penetration sites shown in “B”.

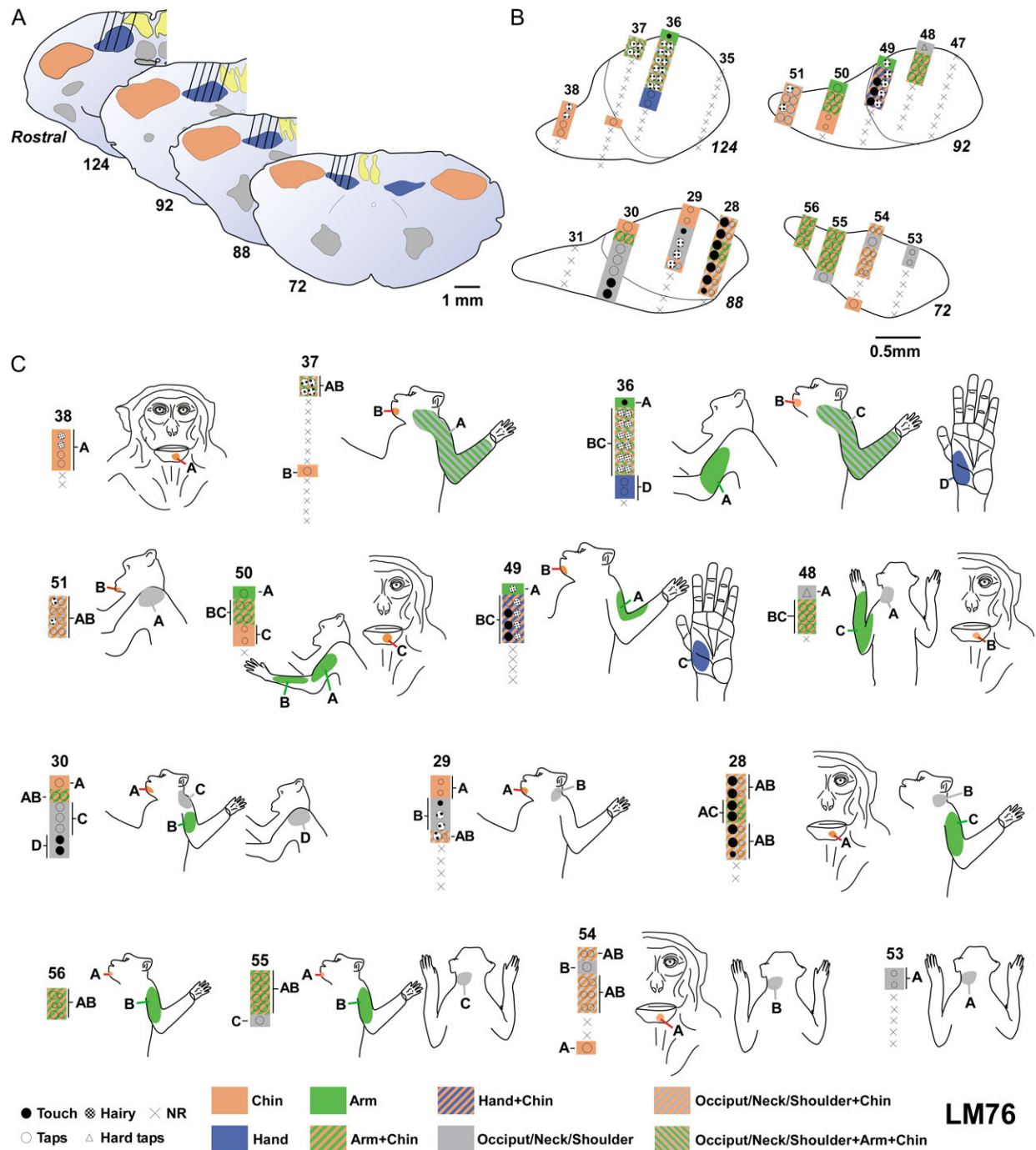


Figure 4. Somatotopy of the cuneate nucleus of monkey LM76 with lesion of the dorsal columns. For reconstruction of the lesion site, see Figure 2A. (A) Outline drawings of a series of sections through the medulla showing cuneate (blue), gracile (yellow) and spinal trigeminal (orange) nuclei. Black vertical lines show locations of representative electrode tracks shown in “B” and “C”. Rostral-most section is in the upper left. Section numbers are marked for reference. (B) Enlarged outline diagrams of the cuneate nucleus showing electrode tracks with locations of the receptive fields on the body and the nature of the neuronal responses at each recording site shown coded as per the key at the bottom. Receptive fields at multiple locations on the body encountered at a recording site are shown with hatches in corresponding colors. (C) Receptive fields of neurons at each recording site for the tracks shown in “B”. Other conventions as for Figure 3.

to touch on the hand, because in this monkey the lesion was partial (Figs 2A and 5; also see Fig. 8C). In other monkeys with less sparing, only at few sites neurons had receptive fields on the hand (Fig. 4). It was hard to discern any somatotopy in the residual digit representations. Receptive fields on the digits were generally larger than normal (Fig. 5C), although neurons continued to respond robustly to light tactile stimulation. However, at many sites the

responses were weaker or required tapping of the skin (see Fig. 4B, Pen #36). At many of the recording sites in the cuneate nucleus we failed to elicit any response to tactile stimulation of any body part. Such nonresponsive sites constituted 23.7% of the 519 recording sites. We did not find any qualitatively obvious differences in the spontaneous activity of neurons or excessive bursting in the firing pattern as compared with the normal animals.

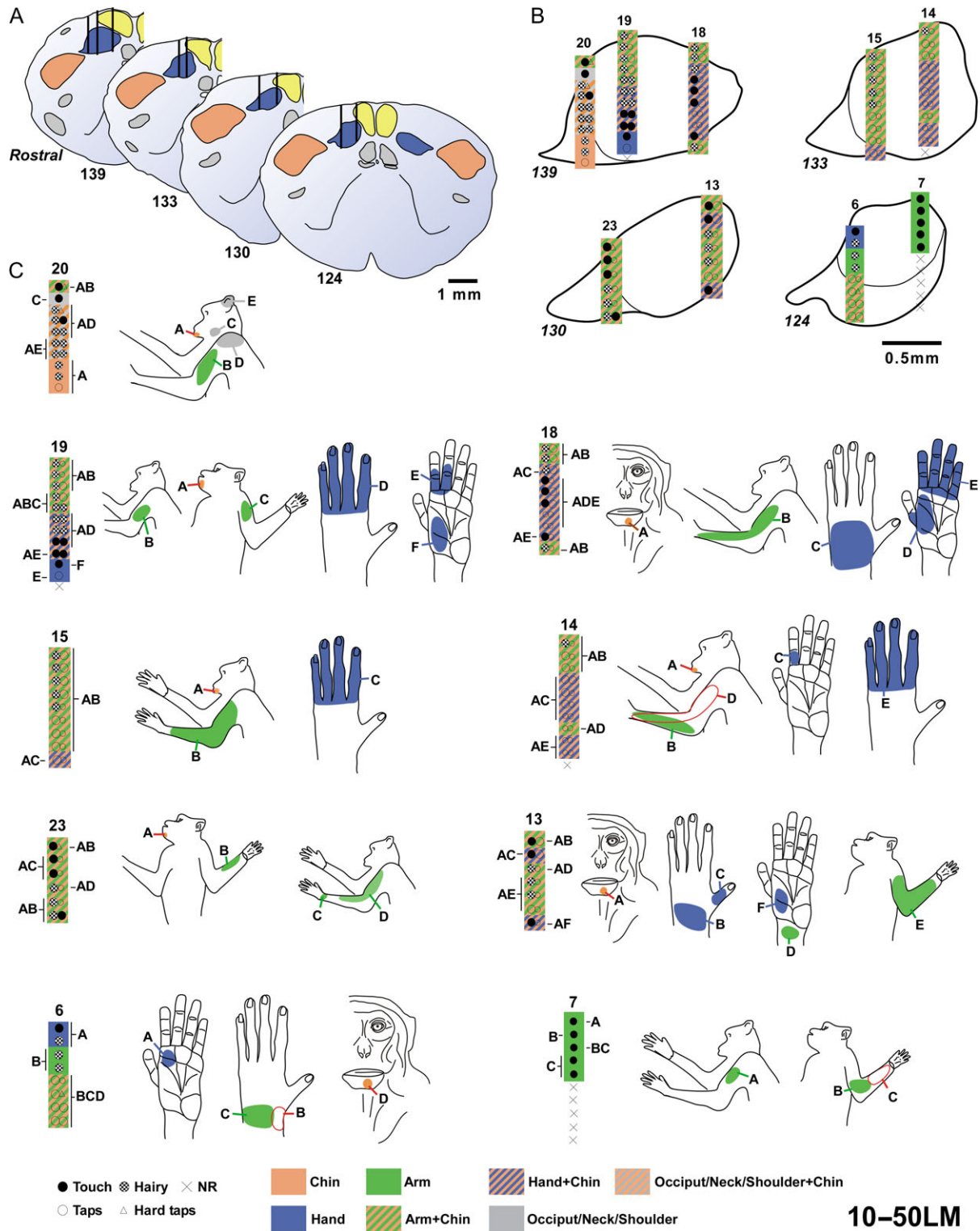


Figure 5. Somatotopy of the cuneate nucleus of monkey 10-50LM with lesion of the dorsal columns. This monkey had considerable sparing of the hand inputs (Fig. 2A). (A) Outline drawings of a series of sections through the medulla showing cuneate (blue), gracile (yellow) and spinal trigeminal (orange) nuclei. Black vertical lines show locations of representative electrode tracks shown in "B" and "C". Rostral-most section is in the upper left. Section numbers are marked for reference. (B) Enlarged outline diagrams of the cuneate nucleus showing electrode tracks with location of the receptive fields on the body and the nature of the neuronal responses at each recording site shown coded as per the key at the bottom. (C) Receptive fields of neurons at each recording site for the tracks shown in "B". Other conventions as for Figures 3 and 4.

One feature of reorganization of the cuneate nucleus was that at majority of the recording sites (51.3%; $n = 396$) neurons had dual receptive fields. Along with the chin, neurons

responded to tactile stimulation of the arm, occiput/neck/shoulder, or the hand. Dual receptive fields, which included hand, were observed in monkeys with sparing of the dorsal column

fibers. At few recording sites (10 out of 396), the receptive fields were on 3 different body regions—chin, arm, and occiput/neck/shoulder (Fig. 4C, Pen #36). Thus after injuries, inputs from multiple sources can have access to the deafferented regions of the cuneate nucleus. We have defined deafferented region as the part of the brain that is expected to lose its normal peripheral inputs, either partially or completely as a result of the injury.

In summary, following spinal cord injuries there is an expansion of the chin representation throughout the cuneate nucleus. Occiput, neck, and shoulder expansion was observed in 3 of the monkeys, but not in monkey 10-50LM with considerable sparing of the inputs. The arm representation had also expanded into the deafferented hand region of the cuneate nucleus.

Somatotopy in the Gracile Nucleus of Monkeys With Lesions

We made 40 penetrations through the gracile nucleus of monkeys with dorsal column lesions and mapped receptive fields of neurons at 236 recording sites. As in the normal monkeys, neurons were responsive to touch on the leg, foot, and tail (Fig. 6; Qi and Kaas 2006). The neurons responded to light tactile stimulation as vigorously as in the normal animals. In addition, in 2 of the monkeys, LM49 and 10-50LM, neurons also responded to touch on the chin at 30.2% of the responsive sites (Fig. 6C, D). Neurons generally responded to taps on the chin or occiput/neck/shoulder and not to light cutaneous stimulation. Furthermore, there was also an expansion of the occiput, neck, and shoulder representations

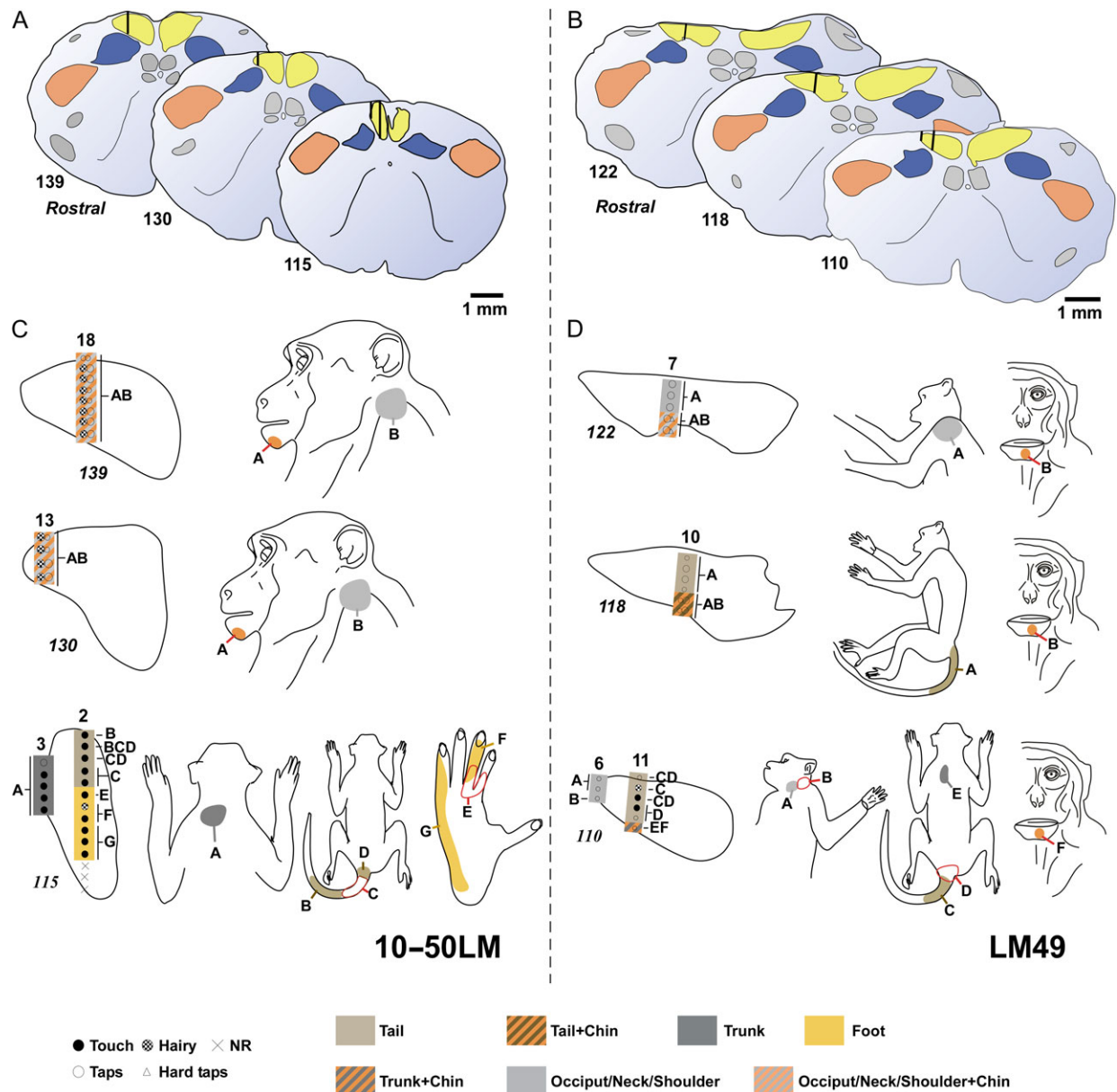


Figure 6. Organization of the gracile nucleus of monkeys 10-50LM and LM49 with lesions of the dorsal columns (Fig. 2). (A and B) Outline drawings of a series of sections through the medulla showing cuneate (blue), gracile (yellow) and spinal trigeminal (orange) nuclei for monkey 10-50LM (A) and LM49 (B). Black vertical lines mark representative electrode tracks shown in “C” and “D”. Rostral-most sections are in the upper left. Section numbers are marked for reference. (C and D) Enlarged outline diagrams of the gracile nuclei of monkeys 10-50LM (C) and LM49 (D) showing electrode tracks with location of the receptive fields on the body and the nature of the neuronal responses at each recording site shown coded as per the key at the bottom. Other conventions as for Figures 3 and 4.

in the gracile nucleus of these 2 monkeys (e.g., Fig. 6C, Pen #18; Fig. 6D). We also observed dual receptive fields such as on the shoulder and chin, or tail and chin (Fig. 6C, Pen #13 and 18; Fig. 6C, Pen #10). No abnormal chin or occiput/neck/shoulder responsive neurons were observed in the gracile nucleus of the other 2 monkeys, LM76 and LM59.

Organization of Area 3b in Monkeys With Dorsal Column Lesions

In normal area 3b, representations of the body parts progress from face to hand, arm, occiput/neck/shoulder, trunk, leg, foot,

and tail in a lateral to medial order. The chin representation is in the ventral part of the face representation, laterally adjacent to the hand-face border (Fig. 7A; Nelson et al. 1980; Pons et al. 1991).

In monkeys with dorsal column lesions the reorganized somatotopy in area 3b was similar to what has been described in detail before (Jain et al. 1997, 2008; Tandon et al. 2009; Dutta et al. 2014; Kambi et al. 2014). In all the monkeys the chin representation had expanded medially into the deafferented hand region up to the medial-most mapped location, which was 6.5–8.6 mm from the hand-face border (Fig. 7C, E). The expanded chin inputs covered the entire deafferented hand representation irrespective of the extent of preserved hand

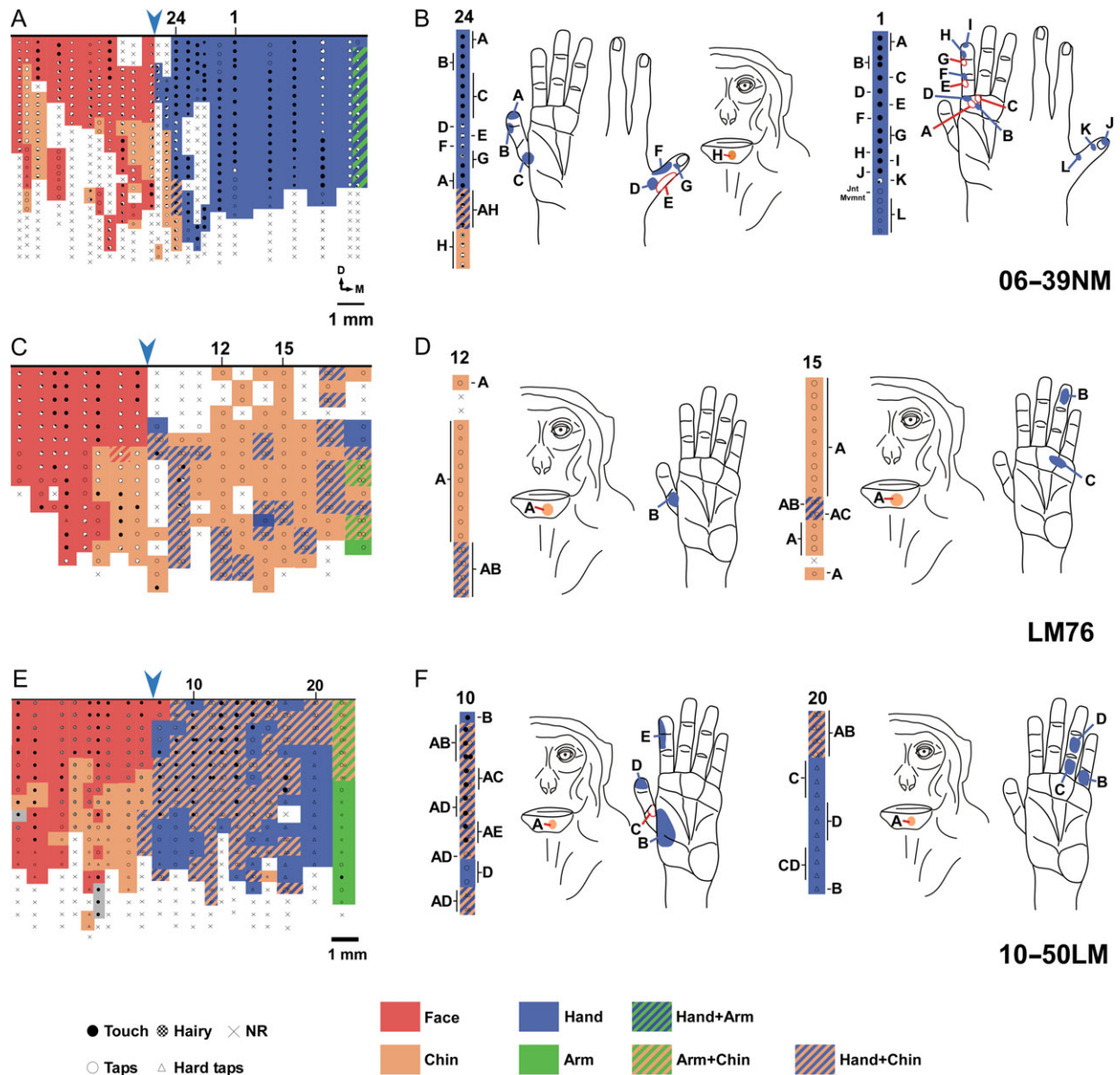


Figure 7. Somatotopy of area 3b of a normal monkey and 2 monkeys with chronic dorsal column injuries. (A) Somatotopy of normal area 3b in monkey 06-39NM. The dots and crosses represent the sites where receptive fields were mapped. Different symbols represent stimulus required to evoke a response (see key at the bottom). Colors represent different body parts where receptive fields were located as per the key at the bottom. The top horizontal line corresponds to a depth of 800 μ m in the sulcus. Blue arrowhead marks location of the hand-face border (see Materials and Methods). Part of the lateral area 3b in this monkey was not mapped due to a fold in the sulcus. (B) Receptive fields along 2 representative electrode tracks for monkey 06-39NM. See the corresponding electrode track numbers in “A”. “Jnt Mvmnt”, joint movement. (C, E) Somatotopy in monkeys LM76 and 10-50LM with dorsal column lesions. Locations where neurons responded to more than one body part are hatched with corresponding colors. Other conventions as for “A”. Data in “C” is shown here for reference from Kambi et al. (2014). (D, F) Representative receptive fields in area 3b for the maps shown in “C” and “E”. See Figure 2A for the extent of the lesion and Figure 3 for other conventions.

representation (see below). For determining the extent of the expansion, normal hand-face border was marked where a perpendicular drawn from tip of the intraparietal sulcus meets the central sulcus (Chand and Jain 2015).

Neuronal responses to the tactile stimulation of the hand were observed in area 3b depending on the extent of sparing of the dorsal column fibers (Fig. 7, also see Figs 2 and 8D). In monkey 10-50LM, where there was considerable sparing, responses to stimulation of the hand were present throughout the partially deafferented hand region. In the other 3 monkeys neurons responded to touch on the hand at few recording sites ranging from only 1 site for monkey LM59 (1.1% of the 88 hand responsive sites), 14.8% for monkey LM49 ($n = 149$), and 36% for monkey LM76 ($n = 111$). In the spared hand representation, the overall progression of somatotopy from D1 to D5 in the lateral to medial direction was preserved (Fig. 7C; Jain et al., 2008; Qi et al. 2011). The receptive fields of neurons in the spared hand representation were sometimes much larger than in the normal animals, often covering more than half of a glabrous digit or the entire palm, although small receptive fields were also observed.

In monkeys with spared hand representation, at many recording sites, the neurons had dual receptive fields on the hand and the chin. For example, in monkey 10-50LM, where the sparing was maximum, dual receptive fields on the hand and chin were present at 66.5% ($n = 158$) of the hand responsive sites. At the remaining hand-responsive sites no response to chin stimulation was elicited, and at one recording site neurons responded exclusively to touch on the chin. In monkey LM49, at all the hand responsive sites neurons had dual receptive fields. In monkey LM76 dual receptive fields were observed at 90% ($n = 40$) of the hand responsive sites; while in monkey LM59 that had receptive field on the hand at only one site at which neurons did not respond to touch on the chin. Thus, neurons in the partially deafferented area 3b hand acquired receptive fields on the chin even if they continue to receive inputs from the hand.

Medially we mapped area 3b until neurons with receptive fields on the arm were encountered. Of the 44 responsive sites where neurons had receptive fields on the arm, we found dual receptive fields on the chin and arm at 54.5% of the sites. Thus chin representation had expanded into the arm representation and likely even more medially (Jain et al. 1997, 2008).

Comparison of the Receptive Fields in the Cuneate Nucleus and Area 3b of the Lesioned Monkeys

A comparison of the somatotopic reorganization in area 3b and the cuneate nucleus showed that the nature of reorganization in these 2 regions of the brain had many differences. Since in area 3b only the hand region was completely mapped, we focus on comparison with this region.

In the deafferented hand region of area 3b the anomalous receptive fields were present only on the chin (Fig. 8A; also see Fig. 7). Responses to stimulation of the chin were found at 90.1% ($n = 496$) of the responsive sites that were judged to be in the deafferented hand region of the 4 monkeys. At none of the responsive sites neurons responded to touch on the neck/shoulder/occiput or arm. In contrast in the cuneate nucleus both the chin and the occiput/neck/shoulder representations expanded to occupy the deafferented hand region throughout the cuneate nucleus (Fig. 8A, B). In the cuneate nucleus at 75.2% ($n = 396$) of the responsive sites neurons responded to touch on the chin; and at 31.5% of the sites the receptive fields were on

occiput, neck, or shoulder (Fig. 8B). An expansion of the arm representation also took place in both the cuneate nucleus and area 3b (Jain et al. 1997, 2008), although the precise extent of its expansion is hard to estimate.

If the lesion was partial, neurons also responded to touch on the hand in both area 3b and the cuneate nucleus depending upon the extent of sparing of the dorsal columns (Fig. 8C, D). The percentage of sites where hand receptive fields were found had a similar trend across monkeys in area 3b and the cuneate nucleus (Fig. 8E). The extent of remaining hand responses between the cuneate nucleus and area 3b was highly correlated ($R^2 = 0.982$; $P = 0.0089$; Fig. 8E). The results suggest that in both, the cuneate nucleus and area 3b, the extent of remaining hand inputs are strongly related to the extent of remaining dorsal column fibers.

A second related feature of reorganization in the cuneate nucleus was presence of anomalous receptive fields on 2 different body parts at the same recording site. At 40.9% ($n = 396$) of all the responsive sites in the cuneate nucleus, dual receptive fields were observed on the chin and occiput/neck/shoulder or arm. Thus in the cuneate nucleus, chin, occiput/neck/shoulder, and arm representations expand to occupy the same territory in the deafferented hand region, whereas in the hand region of area 3b, the only expanded representation was chin (Fig. 8D).

Thus in monkeys with chronic lesions of the dorsal columns, reorganization in area 3b and the cuneate nucleus is similar to the extent that both these region show extensive expansion of the chin inputs in the deafferented hand representation. However, unlike area 3b, in the cuneate nucleus there is also an expansion of the occiput/neck/shoulder and arm that reactivate the deafferented neurons.

Discussion

Major findings of our study are: (1) following unilateral lesions of the dorsal columns of the spinal cord at cervical levels in adult macaque monkeys there is a large-scale expansion of the face inputs into the cuneate nucleus, similar to that observed in area 3b; (2) unlike the hand region of area 3b, an expansion of the occiput, neck, and shoulder representations takes place in the cuneate nucleus; and (3) expansion of the chin and occiput/neck/shoulder representations sometimes extends into the gracile nucleus. Below we discuss our results focusing on reports from adult primates after describing technical limitations of the study.

Technical Limitations of the Study

Multineuron extracellular recordings used in this study is a robust technique to determine somatotopy of large areas of the brain. However, since we did not record responses of isolated single units, it is not possible to determine if responses to multiple body parts at a recording site are because different neurons respond to different body parts, or all or some of the neurons respond to multiple body parts.

Secondly, we have performed experiments under ketamine and xylazine anesthesia, which has been supplemented by urethane. This anesthetic regime has been used in a large number of studies from our lab and in other labs (Merzenich et al. 1983; Jain et al. 2008; Bowes et al. 2012). Ketamine and xylazine have been shown not to generally affect overall somatotopy (Stryker et al. 1987).

Finally, we have not quantitatively compared the nonresponsive sites across monkeys, or between the cuneate nucleus

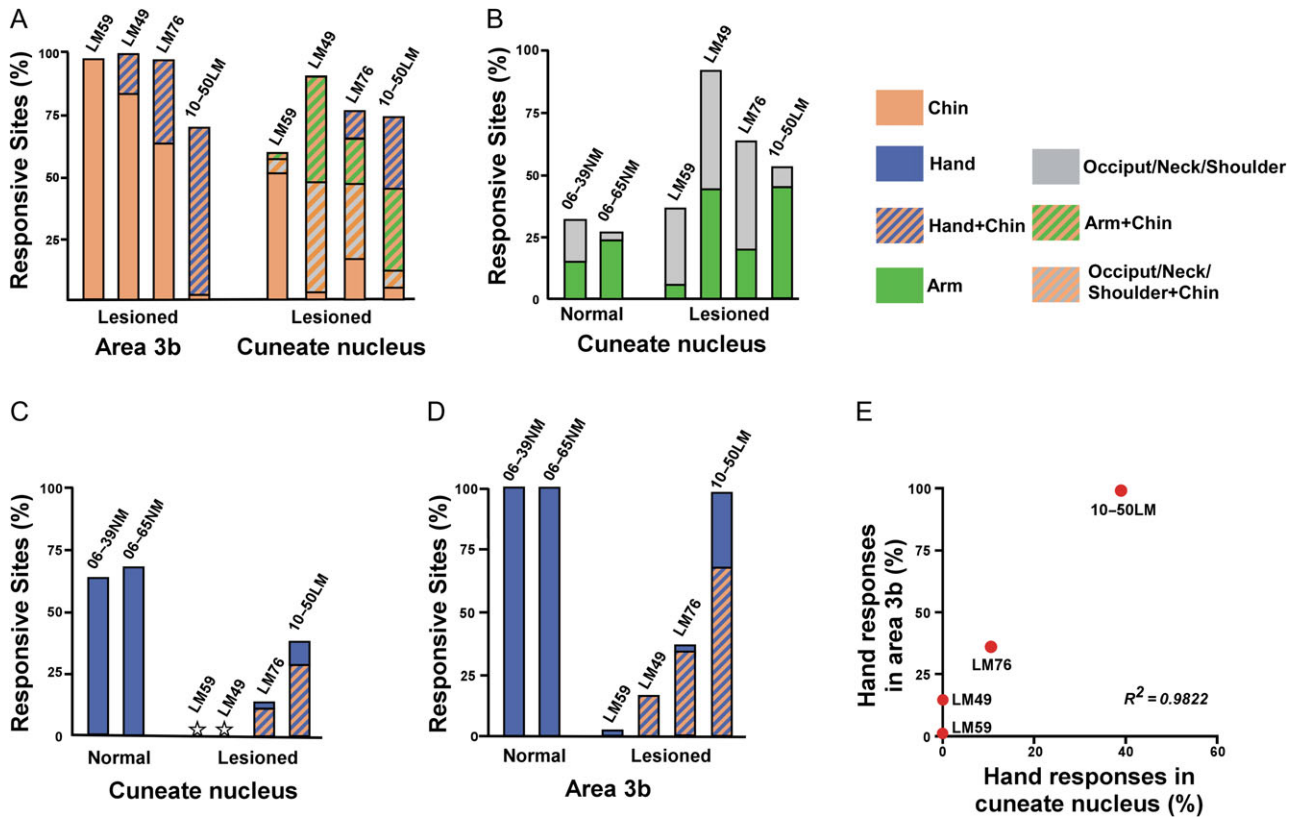


Figure 8. Bar graphs showing percentage of responsive sites with receptive fields on different body parts in area 3b and cuneate nucleus of the normal and lesioned monkeys. (A) Percentage of responsive sites with receptive fields on the chin in the hand region of area 3b and the cuneate nucleus of the monkeys with dorsal column lesions. Recording sites with receptive fields on the chin and another body part are shown color coded as per the key on the right. The monkey numbers are shown on top of the bars. (B) Percentage of responsive sites with receptive fields on the arm and occiput/neck/shoulder in the cuneate nucleus of the normal and lesioned monkeys. There is an enlargement of these representations in the lesioned monkeys. The percentages shown are for the entire cuneate nucleus, that is, it includes both pars rotunda and pars triangularis. (C) Percentage of responsive sites with receptive fields on the hand in the cuneate nucleus of the 2 normal and the 4 lesioned monkeys. Stars indicate that there were no receptive fields on the hand in the cuneate nucleus of monkeys LM59 and LM49. For the lesioned monkeys, recording sites with dual receptive fields on both the hand and the chin are also shown. See the color key. (D) Percentage of responsive sites with receptive fields on the hand in the hand region of area 3b of the normal monkeys and the monkeys with dorsal column lesions. (E) A scatter plot showing correlation between the remaining hand responsive sites in the cuneate nucleus and in area 3b in monkeys with dorsal column lesions.

and area 3b. This is because it is hard, particularly in area 3b, to establish that neurons at a recording site are nonresponsive to peripheral stimulation because the electrode tip is not at an optimal location in the folded depths of posterior bank of the central sulcus and not due to an absence of the inputs. Location of the tip of the electrode can at best only be approximated unless all the recording sites and tracks are marked by electrolytic lesion, an extremely difficult task for a large number of recording sites. For the same reason, we have not separately quantified responsive sites according to the vigorosity of the response or the nature of stimulus required. Even in the cuneate nucleus these parameters can be affected by location of the electrode tip with respect to CO-dark patches, which receive most of the peripheral afferents (Florence et al. 1989). Therefore, we have described only the overall qualitative impression of the nature of responses, and detailed data is illustrated in the figures.

Reorganization and the Nature of Emergent Receptive Fields at Different Levels of the Somatosensory Network

Reorganization at multiple levels in the somatosensory pathway takes place following deafferentations in monkeys, humans, and other mammalian species (Kaas 1991, 2002; Buonomano and

Merzenich 1998; Jones 2000; Jain and Tandon 2012). Most comprehensive description of the nature of reorganization is available for monkeys with deafferentation due to transection of the median and ulnar nerves. Following such injuries neurons in the deafferented hand region in the cuneate nucleus, VPL and area 3b get activated by radial nerve inputs from the hairy skin on the hand (Garraghty and Kaas 1991; Churchill et al. 2001). Similarly, deafferentation by amputation of the digits leads to expansion of inputs from the stump and neighboring intact digits in area 3b and VPL of monkeys and humans (Merzenich et al. 1984; Florence and Kaas 1995; Davis et al. 1998; Florence et al. 1998; Weiss et al. 1998). Deafferented neurons in the cuneate nucleus also come to respond to touch in the borders of the deprived zone following long-term deafferentation by cutting of dorsal roots innervating digits D1–D3 (Darian-Smith and Ciferrì 2006).

Large deafferentations that result in expansion of face representation into the deafferented hand region of area 3b also lead to subcortical plasticity. In macaque monkeys with transection of the dorsal roots from C2 to T1 performed 10–21 years prior to mapping, neurons in both the deafferented area 3b and VPL acquire responses to touch on the face (Pons et al. 1991; Jones and Pons 1998). No major differences were reported in the nature of receptive fields in the reorganized VPL and area 3b. Similarly, expansion of the chin inputs is seen in area 3b, VPL

and cuneate nucleus of monkeys with chronic lesions of the dorsal columns at cervical levels (this report; Jain et al. 1997; Jain et al. 2008; Tandon et al. 2009; Qi et al. 2011; Dutta et al. 2014).

Here we report that in the deafferented cuneate nucleus neurons acquire receptive fields on the occiput, shoulder and neck, in addition to the chin (Fig. 9). Receptive fields on the occiput/shoulder/neck were not observed in the deafferented hand region of area 3b in any of our monkeys or those reported previously following different kinds of deafferentations, (Pons et al. 1991; Florence and Kaas 1995; Jain et al. 1997, 2008; Florence et al. 2000).

Occiput, shoulder and the neck are innervated by the rostral-most cervical nerves II–V (Sherrington 1939; Nelson et al. 1980). In the cuneate nucleus occiput/shoulder/neck representations are in somatotopic order, between the hand representations medially and the face representation in the trigeminal nucleus laterally (Edney and Porter 1986; Xu and Wall 1999b). However, in area 3b of monkeys these body part representations are medial to the forelimb representation, which is innervated by cervical nerves VI–VIII. Thus there is a rearrangement of somatotopic order of the spinal nerve inputs as they ascend from the brainstem nuclei to area 3b (CN Woolsey as

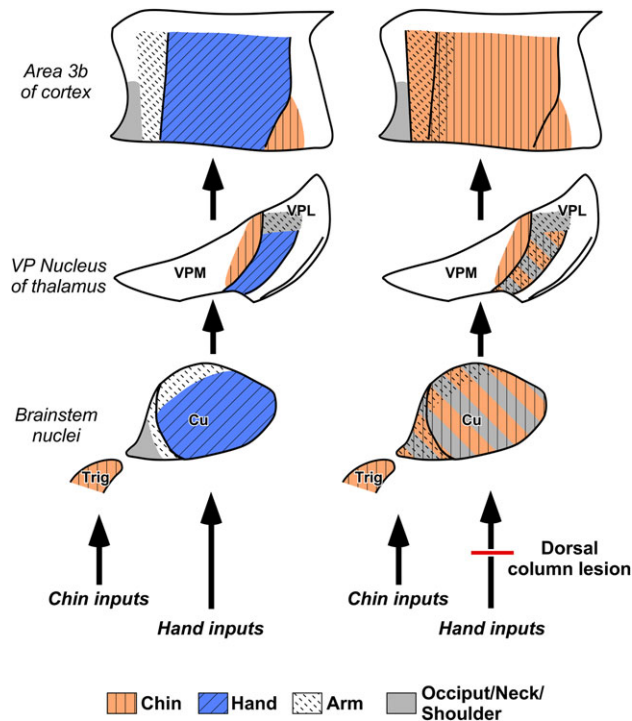


Figure 9. A summary diagram showing reorganization at different levels in the somatosensory system following dorsal column lesions. (Left) In a normal monkey trigeminal inputs from the chin project to the face region of area 3b via trigeminal nucleus of the brainstem (Trig) and VPM nucleus of the thalamus (Kaas et al. 1984; Rausell and Jones 1991). The hand inputs ascend via the cuneate nucleus (Cu) to the VPM, and from VPM to the hand representation in area 3b. See color key at the bottom. (Right) In monkeys with chronic lesions of the dorsal columns, chin inputs expand into the deafferented hand region of the cuneate nucleus, VPM of the thalamus and area 3b. In the cuneate nucleus (this report) and VPL (Jain et al. 2008) there is also an expansion of the occiput/neck/shoulder and arm inputs, inputs that enter the spinal cord rostral to the lesion. In the hand region of area 3b there is no expansion of occiput/neck/shoulder inputs, although there can be a limited expansion of the arm. If there are any remaining hand inputs because of a partial lesion, those inputs are also observed at all the 3 levels (not shown). Dorsal is towards the top; medial is towards right for the brainstem nuclei, and towards left for the VP nucleus and area 3b.

cited in Dykes and Ruest 1986; Xu and Wall 1999b). The occiput/neck/shoulder and some of the arm inputs enter the spinal cord rostral to the lesions.

Occiput/neck/shoulder representations also expand to occupy the deafferented hand subnucleus of VPL. Jain et al. (2008) mapped both area 3b and VPL in monkeys with chronic dorsal column lesions. They illustrate an expansion of the occiput/neck/shoulder representations as well as chin in the deafferented hand subnucleus of VPL (see Figs 18–22 of Jain et al. 2008). Similarly in a human patient, 5 years after clinically complete transection of the spinal cord at C5 level, neurons at multiple locations in the somatosensory thalamus responded to touch on the occiput/neck/shoulder (Lenz et al. 1987). Thus inputs from occiput/neck/shoulder expand in the cuneate nucleus and VPL but not in area 3b.

Our results also show that there is an expansion of the arm representation in the cuneate nucleus. An expansion of the arm representation has also been reported in the VPL of monkeys with dorsal column injuries (Jain et al. 2008). However, in area 3b, expansion of the arm representation is more limited and is restricted to the medial-most part of the deafferented hand region (Jain et al. 1997; Jain et al. 2008). We also found generally weaker responses to stimulation of the hand in the cuneate nucleus of the 2 monkeys and in area 3b of all the 4 monkeys. While these responses are likely due to intact dorsal column fibers, the second order dorsal column inputs could also contribute to such responses (Liao et al. 2015).

Thus deafferentation-induced emergent receptive fields in the cuneate nucleus are similar to those in VPL. However, receptive fields are selectively expressed in area 3b in a region-specific manner.

Reorganization of the Gracile Nucleus

In 2 monkeys we observed expansion of the chin and occiput/neck/shoulder representations in the nucleus gracilis. We did not map area 3b of these monkeys in the region of the lower limb representation. However, Jain et al. (2008) show data for the entire area 3b of 2 monkeys with chronic dorsal column lesions (their Figs 4 and 12). Interestingly, in 1 of the 2 monkeys neurons in the lower limb region had receptive fields on the occiput/neck/shoulder and chin (their Fig. 12). In the same monkey, the foot subnucleus of VPL neurons had receptive fields on occiput/neck/shoulder as well as chin (their Figs 18–21). In the other monkey in which complete area 3b was mapped, there were no anomalous receptive fields in the medial-most regions of area 3b (their Fig. 4). No data is shown from the foot subnucleus of VPL of this monkey (their Fig. 17). It is not clear why such extensive reorganization of the nucleus gracilis and the corresponding upstream regions in VPL and area 3b is observed only in some of the monkeys with lesions. An examination of the data from our limited sample size did not reveal any correlation with factors such as the extent of the spared dorsal column fibers or the postinjury recovery periods.

Possible Mechanisms of Altered Expression Pattern of Receptive Fields in Area 3b

Receptive fields of neurons are determined by a complex interaction of feedforward, feedback, lateral and callosal connections. The divergence and convergence of projections as well as modulation by excitatory and inhibitory inputs affects neuronal response properties (Alloway and Burton 1991; Clarey et al. 1996; Liao et al. 2013). For example, experiments show that

expression of the normal as well as reorganized receptive fields of neurons in the thalamus depends upon ongoing activity in the somatosensory cortex (Ergenzinger et al. 1998; Krupa et al. 1999; Temereanca and Simons 2004).

As described above, occiput/neck/shoulder representations are adjacent to the hand in the cuneate nucleus and VPL, but not in area 3b. Thus, it appears that occiput/neck/shoulder representation expand into the hand region only if they are the adjacent representations. Interestingly, expansion of the occiput/neck/shoulder region in addition to the chin is also seen in area S2 and PV of monkeys with dorsal column lesions (Tandon et al. 2009). In S2 and PV also the chin as well as occiput/neck/shoulder representations are adjacent to the hand representation (Krubitzer et al. 1995). This requirement for adjacency would suggest the possibility of axonal sprouting into the deprived region, which could take place at each level in the pathway independently. Alternatively, these 2 representations could have an overlapping representation in the cuneate nucleus, VPL, and areas S2 and PV, both of which are not expressed in normal monkeys due to lateral inhibition.

However, the possibility that expansion of occiput/neck/shoulder and arm representations in the cuneate nucleus is because of a pre-existing overlap of these inputs and the hand inputs, which get expressed after neurons lose their primary drive from the hand appears to be unlikely, because the zones of termination of the afferents are confined to small regions. Afferents from skin of the hand and arm terminate in restricted regions in the cuneate nucleus without any overlap (Florence et al. 1989; Florence and Kaas 1995; Wu and Kaas 2002). We did not find any report in the literature examining projection pattern of afferents from the skin of the occiput, neck, or shoulder to the brainstem nuclei, but they could have a similar restricted projection zone (Edney and Porter 1986; Wu and Kaas 2002). The second possibility is that expansion of the occiput/neck/shoulder inputs is due to sprouting of these inputs into the deafferented hand region. At present there is no direct evidence of this growth. However, afferent sprouting has been reported following lesions of the dorsal columns and limb amputations (Jain et al. 2000; Wu and Kaas 2002), or following partial hand deafferentation (Darian-Smith 2004). We have previously shown that expression of chin inputs in the deafferented hand region of area 3b and possibly VPL depends entirely upon reorganization of the cuneate nucleus, which is likely due sprouting (Kambi et al. 2014; Jain et al. 2000).

Receptive fields on occiput/neck/shoulder in the deafferented hand subnucleus of VPL can be an upstream expression of reorganization in the cuneate nucleus via pre-existing topographic cuneothalamic connections (Boivie 1978; Berkley 1980; Kaas et al. 1999; for physiological evidence see Kambi et al. 2014). Alternatively, occiput/neck/shoulder can also independently reactivate the adjacent deafferented hand neurons by sprouting or expression of latent pre-existing connections. Occiput neck and shoulder representations are located adjacent to the hand representation in VPL, both dorsally as well as in the lateral-most part of the hand subnucleus (Mountcastle and Henneman 1952; Jones and Friedman 1982a; Kaas et al. 1984).

However, it is puzzling why occiput/neck/shoulder receptive fields of the neurons in the deafferented hand subnucleus of VPL are not expressed in the hand region of area 3b via pre-existing connections between VPL and area 3b (Jones and Friedman 1982b; Rausell et al. 1998; Liao et al. 2013; Chand and Jain 2015). Therefore, our findings suggest that active mechanisms must exist to selectively suppress expression of occiput/neck/shoulder inputs in the deafferented hand region of area

3b. We propose that this is regulated in VPL as the thalamocortical inputs ascend to area 3b.

GABAergic inhibition could possibly mediate selective expression of only the chin inputs in the hand region of area 3b. GABAergic inhibition has been shown to play a role in suppressing expression of reorganized somatotopy of the cuneate nucleus in the primary somatosensory cortex of rats with neonatal limb amputation (Lane et al. 1997). Changes in the GABA mediated inhibition has been proposed to play a role in deafferentation-induced plasticity (Garraghty et al. 1991; Levy et al. 2002). There are 2 sources of GABAergic inhibition in macaque thalamus that help shape the ascending inputs. Ascending medial lemniscal inputs synapse on the thalamocortical projection neurons as well as on the inhibitory interneurons, which form a synaptic triad (Ralston and Ralston 1994; Ralston et al. 1996). In addition, corticothalamic neurons pass through the reticular nucleus where they give off collaterals on GABAergic reticular neurons, which presumably also have access to the ascending thalamocortical fibers (Lee et al. 1994a, b; Temereanca and Simons 2004; Crandall et al. 2015).

One possibility is that in addition to their normal targets, some of the ascending occiput/neck/shoulder inputs also terminate in the hand subnucleus of VPL. In normal monkeys a strong drive from the hand suppresses expression of these occiput/neck/shoulder inputs by GABAergic inhibition via the circuits described above. However, neurons that receive primary drive from the hand inputs project to the hand region of area 3b, and those from occiput/neck/shoulder to the corresponding region in area 3b. Our preliminary unpublished experiments suggest that thalamocortical neurons projecting to occiput/neck/shoulder representations in area 3b are present in at least parts of the hand subnucleus of VPL. In the deafferented monkeys with reorganized VPL, the weaker drive from the expanded chin inputs is not able to exert the same level of inhibitory influence, resulting in expression of the occiput/neck/shoulder inputs in the hand subnucleus of VPL. However, these are not expressed in the hand region of area 3b because of the specific projection pattern. Previously, reduced drive from the cuneate nucleus has been reported to reduce GABA in VPL, thus reducing inhibition (Ralston et al. 1996).

Dual receptive fields on the arm and chin, and arm and occiput/neck/shoulder were observed in area 3b, cuneate nucleus and VPL (Jain et al. 2008). Dual receptive fields on different parts of the hand have also been reported following regeneration of surgically repaired nerve cuts (Wall and Kaas 1986; Wall et al. 1986). In monkeys with dorsal column lesions dual receptive fields also include the hand in case of partial deafferentations. Presence of dual receptive fields suggests that even partial deafferentation can trigger complex reactive mechanisms to permit deafferented neurons at the same location to be accessed by multiple intact inputs as discussed above. Moreover, deafferentations such as amputations, lead to perception of a phantom limb when either the stump or the chin is touched (Ramachandran 1993). The dual receptive fields of the deafferented neurons that emerge following brain reorganization could underlie perception of a phantom by touch on more than one part of the body.

Funding

Department of Biotechnology, Government of India to N.J. (No. BT/PR7180/MED/30/907/2012) and core funds from National Brain Research Centre. CSIR-UGC Junior Research Fellowship (No. 19-06/2011(i)EU-IV) to P.H. from the Council of Scientific

and Industrial Research, Government of India. Research Associate Fellowship from Council for Scientific and Industrial Research (No. 9/821(0034)/2011-EMR-1) to P.C.

Notes

Authors fondly remember Mr Vasav Arora who contributed to this work but is unfortunately not with us to see it published. We also thank Shashank Tandon, Radhika Rajan, Leslee Lazar, and Hisham Mohammed for help with some of the electrophysiology experiments and surgical procedures. Mr Mithlesh Singh and Mr Hari Shankar provided histological and other support. Thanks to Dr V. Rema for helpful comments on the article. *Conflict of Interest:* None declared.

References

- Alloway KD, Burton H. 1991. Differential effects of GABA and bicuculline on rapidly- and slowly-adapting neurons in primary somatosensory cortex of primates. *Exp Brain Res.* 85: 598–610.
- Berkley KJ. 1980. Spatial relationships between the terminations of somatic sensory and motor pathways in the rostral brainstem of cats and monkeys. I. Ascending somatic sensory inputs to lateral diencephalon. *J Comp Neurol.* 193:283–317.
- Boivie J. 1978. Anatomical observations on the dorsal column nuclei, their thalamic projection and the cytoarchitecture of some somatosensory thalamic nuclei in the monkey. *J Comp Neurol.* 178:17–48.
- Bowes C, Massey JM, Burish M, Cerkevich CM, Kaas JH. 2012. Chondroitinase ABC promotes selective reactivation of somatosensory cortex in squirrel monkeys after a cervical dorsal column lesion. *Proc Natl Acad Sci USA.* 109: 2595–2600.
- Buonomano DV, Merzenich MM. 1998. Cortical plasticity: from synapses to maps. *Annu Rev Neurosci.* 21:149–186.
- Calford MB, Tweedale R. 1988. Immediate and chronic changes in responses of somatosensory cortex in adult flying-fox after digit amputation. *Nature.* 332:446–448.
- Chand P, Jain N. 2015. Intracortical and thalamocortical connections of the hand and face representations in somatosensory area 3b of macaque monkeys and effects of chronic spinal cord injuries. *J Neurosci.* 35:13475–13486.
- Churchill JD, Arnold LL, Garraghty PE. 2001. Somatotopic reorganization in the brainstem and thalamus following peripheral nerve injury in adult primates. *Brain Res.* 910:142–152.
- Clarey JC, Tweedale R, Calford MB. 1996. Interhemispheric modulation of somatosensory receptive fields: evidence for plasticity in primary somatosensory cortex. *Cereb Cortex.* 6: 196–206.
- Corbetta M, Burton H, Sinclair RJ, Conturo TE, Akbudak E, McDonald JW. 2002. Functional reorganization and stability of somatosensory-motor cortical topography in a tetraplegic subject with late recovery. *Proc Natl Acad Sci USA.* 99: 17066–17071.
- Crandall SR, Cruikshank SJ, Connors BW. 2015. A corticothalamic switch: controlling the thalamus with dynamic synapses. *Neuron.* 86:768–782.
- Darian-Smith C. 2004. Primary afferent terminal sprouting after a cervical dorsal rootlet section in the macaque monkey. *J Comp Neurol.* 470:134–150.
- Darian-Smith C, Ciferri M. 2006. Cuneate nucleus reorganization following cervical dorsal rhizotomy in the macaque monkey: its role in the recovery of manual dexterity. *J Comp Neurol.* 498:552–565.
- Davis KD, Kiss ZHT, Luo L, Tasker RR, Lozano AM, Dostrovsky JO. 1998. Phantom sensations generated by thalamic microstimulation. *Nature.* 391:385–387.
- Dostrovsky JO, Millar J, Wall PD. 1976. The immediate shift of afferent drive to dorsal column nucleus cells following deafferentation: a comparison of acute and chronic deafferentation in gracile nucleus and spinal cord. *Exp Neurol.* 52: 480–495.
- Dutta A, Kambi N, Raghunathan P, Khushu S, Jain N. 2014. Large-scale reorganization of the somatosensory cortex of adult macaque monkeys revealed by fMRI. *Brain Struct Funct.* 219:1305–1320.
- Dykes RW, Craig AD. 1998. Control of size and excitability of mechanosensory receptive fields in dorsal column nuclei by homolateral dorsal horn neurons. *J Neurophysiol.* 80: 120–129.
- Dykes RW, Ruest A. 1986. What makes a map in somatosensory cortex? New York: Plenum Press.
- Edney DP, Porter JD. 1986. Neck muscle afferent projections to the brainstem of the monkey: implications for the neural control of gaze. *J Comp Neurol.* 250:389–398.
- Ergenzinger ER, Glasier MM, Hahm JO, Pons TP. 1998. Cortically induced thalamic plasticity in the primate somatosensory system. *Nat Neurosci.* 1:226–229.
- Florence SL, Hackett TA, Strata F. 2000. Thalamic and cortical contributions to neural plasticity after limb amputation. *J Neurophysiol.* 83:3154–3159.
- Florence SL, Kaas JH. 1995. Large-scale reorganization at multiple levels of the somatosensory pathway follows therapeutic amputation of the hand in monkeys. *J Neurosci.* 15: 8083–8095.
- Florence SL, Wall JT, Kaas JH. 1989. Somatotopic organization of inputs from the head to the spinal gray and cuneate nucleus of monkeys with observations on the cuneate nucleus of humans. *J Comp Neurol.* 286:48–70.
- Florence SL, Taub HB, Kaas JH. 1998. Large-scale sprouting of cortical connections after peripheral injury in adult macaque monkeys. *Science.* 282:1117–1121.
- Garraghty PE, Kaas JH. 1991. Functional reorganization in adult monkey thalamus after peripheral nerve injury. *Neuroreport.* 2:747–750.
- Garraghty PE, LaChica AE, Kaas JH. 1991. Injury-induced reorganization of somatosensory cortex is accompanied by reductions in GABA staining. *Somat Mot Res.* 8:347–354.
- Graziano A, Jones EG. 2009. Early withdrawal of axons from higher centers in response to peripheral somatosensory denervation. *J Neurosci.* 29:3738–3748.
- Grüsser SM, Mühlnickel W, Schaefer M, Villringer K, Christmann C, Koeppel C, Flor H. 2004. Remote activation of referred phantom sensation and cortical reorganization in human upper extremity amputees. *Exp Brain Res.* 154: 97–102.
- Jain N, Catania KC, Kaas JH. 1997. Deactivation and reactivation of somatosensory cortex after dorsal spinal cord injury. *Nature.* 386:495–498.
- Jain N, Catania KC, Kaas JH. 1998. A histologically visible representation of the fingers and palm in primate area 3b and its immutability following long-term deafferentations. *Cereb Cortex.* 8:227–236.
- Jain N, Florence SL, Qi HX, Kaas JH. 2000. Growth of new brainstem connections in adult monkeys with massive sensory loss. *Proc Natl Acad Sci USA.* 97:5546–5550.

- Jain N, Qi HX, Collins CE, Kaas JH. 2008. Large-scale reorganization in the somatosensory cortex and thalamus after sensory loss in macaque monkeys. *J Neurosci*. 28:11042–11060.
- Jain N, Tandon S. 2012. Plasticity of the somatosensory system following spinal and peripheral injuries. In: Tandon PN, Tripathi RC, Srinivasan N, editors. *Expanding horizons of the mind sciences*. New York: Nova Science Publishers. p. 93–104.
- Jones EG. 2000. Cortical and subcortical contributions to activity-dependent plasticity in primate somatosensory cortex. *Annu Rev Neurosci*. 23:1–37.
- Jones EG, Friedman DP. 1982a. Projection pattern of functional components of thalamic ventrobasal complex on monkey somatosensory cortex. *J Neurophysiol*. 48:521–544.
- Jones EG, Friedman DP. 1982b. Projection pattern of functional components of thalamic ventrobasal complex on monkey somatosensory cortex. *J Neurophysiol*. 48:521–544.
- Jones EG, Pons TP. 1998. Thalamic and brainstem contributions to large-scale plasticity of primate somatosensory cortex. *Science*. 282:1121–1125.
- Kaas JH. 1991. Plasticity of sensory and motor maps in adult mammals. *Annu Rev Neurosci*. 14:137–167.
- Kaas JH. 2002. Sensory loss and cortical reorganization in mature primates. *Prog Brain Res*. 138:167–176.
- Kaas JH, Nelson RJ, Sur M, Dykes RW, Merzenich MM. 1984. The somatotopic organization of the ventroposterior thalamus of the squirrel monkey, *Saimiri sciureus*. *J Comp Neurol*. 226:111–140.
- Kaas JH, Florence SL, Jain N. 1999. Subcortical contributions to massive cortical reorganizations. *Neuron*. 22:657–660.
- Kaas JH, Qi HX, Burish MJ, Gharbawie OA, Onifer SM, Massey JM. 2008. Cortical and subcortical plasticity in the brains of humans, primates, and rats after damage to sensory afferents in the dorsal columns of the spinal cord. *Exp Neurol*. 209:407–416.
- Kambi N, Tandon S, Mohammed H, Lazar L, Jain N. 2011. Reorganization of the primary motor cortex of adult macaque monkeys after sensory loss resulting from partial spinal cord injuries. *J Neurosci*. 31:3696–3707.
- Kambi N, Halder P, Rajan R, Arora V, Chand P, Arora M, Jain N. 2014. Large-scale reorganization of the somatosensory cortex following spinal cord injuries is due to brainstem plasticity. *Nat Commun*. 5:3602.
- Kerr FW, Kruger L, Schwassmann HO, Stern R. 1968. Somatotopic organization of mechanoreceptor units in the trigeminal nuclear complex of the macaque. *J Comp Neurol*. 134:127–144.
- Krubitzer L, Clarey J, Tweedale R, Elston G, Calford M. 1995. A redefinition of somatosensory areas in the lateral sulcus of macaque monkeys. *J Neurosci*. 15:3821–3839.
- Krupa DJ, Ghazanfar AA, Nicolelis MA. 1999. Immediate thalamic sensory plasticity depends on corticothalamic feedback. *Proc Natl Acad Sci USA*. 96:8200–8205.
- Lane RD, Killackey HP, Rhoades RW. 1997. Blockade of GABAergic inhibition reveals reordered cortical somatotopic maps in rats that sustained neonatal forelimb removal. *J Neurophysiol*. 77:2723–2735.
- Lee SM, Friedberg MH, Ebner FF. 1994a. The role of GABA-mediated inhibition in the rat ventral posterior medial thalamus. I. Assessment of receptive field changes following thalamic reticular nucleus lesions. *J Neurophysiol*. 71:1702–1715.
- Lee SM, Friedberg MH, Ebner FF. 1994b. The role of GABA-mediated inhibition in the rat ventral posterior medial thalamus. II. Differential effects of GABAA and GABAB receptor antagonists on responses of VPM neurons. *J Neurophysiol*. 71:1716–1726.
- Lenz FA, Tasker RR, Dostrovsky JO, Kwan HC, Gorecki J, Hirayama T, Murphy JT. 1987. Abnormal single-unit activity recorded in the somatosensory thalamus of a quadriplegic patient with central pain. *Pain*. 31:225–236.
- Levy LM, Ziemann U, Chen R, Cohen LG. 2002. Rapid modulation of GABA in sensorimotor cortex induced by acute deafferentation. *Ann Neurol*. 52:755–761.
- Liao CC, Gharbawie OA, Qi H, Kaas JH. 2013. Cortical connections to single digit representations in area 3b of somatosensory cortex in squirrel monkeys and prosimian galagos. *J Comp Neurol*. 521:3768–3790.
- Liao CC, DiCarlo GE, Gharbawie OA, Qi HX, Kaas JH. 2015. Spinal cord neuron inputs to the cuneate nucleus that partially survive dorsal column lesions: a pathway that could contribute to recovery after spinal cord injury. *J Comp Neurol*. 523:2138–2160.
- Liao CC, Qi HX, Reed JL, Miller DJ, Kaas JH. 2016a. Congenital foot deformation alters the topographic organization in the primate somatosensory system. *Brain Struct Funct*. 221:383–406.
- Liao CC, Reed JL, Kaas JH, Qi HX. 2016b. Intracortical connections are altered after long-standing deprivation of dorsal column inputs in the hand region of area 3b in squirrel monkeys. *J Comp Neurol*. 524:1494–1526.
- Merzenich MM, Kaas JH, Wall J, Nelson RJ, Sur M, Felleman D. 1983. Topographic reorganization of somatosensory cortical areas 3b and 1 in adult monkeys following restricted deafferentation. *Neuroscience*. 8:33–55.
- Merzenich MM, Nelson RJ, Stryker MP, Cynader MS, Schoppmann A, Zook JM. 1984. Somatosensory cortical map changes following digit amputation in adult monkeys. *J Comp Neurol*. 224:591–605.
- Mountcastle VB, Henneman E. 1952. The representation of tactile sensibility in the thalamus of the monkey. *J Comp Neurol*. 97:409–439.
- Nelson RJ, Sur M, Felleman DJ, Kaas JH. 1980. Representations of the body surface in postcentral parietal cortex of *Macaca fascicularis*. *J Comp Neurol*. 192:611–643.
- Pluto CP, Lane RD, Rhoades RW. 2004. Local GABA receptor blockade reveals hindlimb responses in the SI forelimb-stump representation of neonatally amputated rats. *J Neurophysiol*. 92:372–379.
- Pons TP, Garraghty PE, Ommaya AK, Kaas JH, Taub E, Mishkin M. 1991. Massive cortical reorganization after sensory deafferentation in adult macaques. *Science*. 252:1857–1860.
- Qi HX, Chen LM, Kaas JH. 2011. Reorganization of somatosensory cortical areas 3b and 1 after unilateral section of dorsal columns of the spinal cord in squirrel monkeys. *J Neurosci*. 31:13662–13675.
- Qi HX, Kaas JH. 2006. Organization of primary afferent projections to the gracile nucleus of the dorsal column system of primates. *J Comp Neurol*. 499:183–217.
- Ralston HJ, Ohara PT, Meng X, Wells J, Ralston D. 1996. Transneuronal changes of the inhibitory circuitry in the macaque somatosensory thalamus following lesions of the dorsal column nuclei. *J Comp Neurol*. 371:325–335.
- Ralston HJ, Ralston DD. 1994. Medial lemniscal and spinal projections to the macaque thalamus: an electron microscopic study of differing GABAergic circuitry serving thalamic somatosensory mechanisms. *J Neurosci*. 14:2485–2502.
- Ramachandran VS. 1993. Behavioral and magnetoencephalographic correlates of plasticity in the adult human brain. *Proc Natl Acad Sci USA*. 90:10413–10420.

- Rausell E, Jones EG. 1991. Histochemical and immunocytochemical compartments of the thalamic VPM nucleus in monkeys and their relationship to the representational map. *J Neurosci.* 11:210–225.
- Rausell E, Bickford L, Manger PR, Woods TM, Jones EG. 1998. Extensive divergence and convergence in the thalamocortical projection to monkey somatosensory cortex. *J Neurosci.* 18:4216–4232.
- Saadon-Grosman N, Tal Z, Itshayek E, Amedi A, Arzy S. 2015. Discontinuity of cortical gradients reflects sensory impairment. *Proc Natl Acad Sci USA.* 112:16024–16029.
- Sherrington C. 1939. On the distribution of the sensory nerve roots. In: Denny-Brown D, editor. *Selected writings of Sir Charles Sherrington.* London: Hamish Hamilton Medical Books. p. 31–93.
- Strata F, Coq JO, Kaas JH. 2003. The chemo- and somatotopic architecture of the Galago cuneate and gracile nuclei. *Neuroscience.* 116:831–850.
- Stryker MP, Jenkins WM, Merzenich MM. 1987. Anesthetic state does not affect the map of the hand representation within area 3b somatosensory cortex in owl monkey. *J Comp Neurol.* 258:297–303.
- Tandon S, Kambi N, Lazar L, Mohammed H, Jain N. 2009. Large-scale expansion of the face representation in somatosensory areas of the lateral sulcus after spinal cord injuries in monkeys. *J Neurosci.* 29:12009–12019.
- Temereanca S, Simons DJ. 2004. Functional topography of corticothalamic feedback enhances thalamic spatial response tuning in the somatosensory whisker/barrel system. *Neuron.* 41:639–651.
- Turnbull BG, Rasmusson DD. 1991. Chronic effects of total or partial digit denervation on raccoon somatosensory cortex. *Somatosens Mot Res.* 8:201–213.
- Wall JT, Kass JH. 1986. Long-term cortical consequences of reinnervation errors after nerve regeneration in monkeys. *Brain Res.* 372:400–404.
- Wall JT, Kaas JH, Sur M, Nelson RJ, Felleman DJ, Merzenich MM. 1986. Functional reorganization in somatosensory cortical areas 3b and 1 of adult monkeys after median nerve repair: possible relationships to sensory recovery in humans. *J Neurosci.* 6:218–233.
- Weiss T, Miltner WH, Dillmann J, Meissner W, Huonker R, Nowak H. 1998. Reorganization of the somatosensory cortex after amputation of the index finger. *Neuroreport.* 9:213–216.
- Wilson NR, Runyan CA, Wang FL, Sur M. 2012. Division and subtraction by distinct cortical inhibitory networks in vivo. *Nature.* 488:343–348.
- Wu CW, Kaas JH. 2002. The effects of long-standing limb loss on anatomical reorganization of the somatosensory afferents in the brainstem and spinal cord. *Somatosens Motor Res.* 19:153–163.
- Xu J, Wall JT. 1996. Cutaneous representations of the hand and other body parts in the cuneate nucleus of a primate, and some relationships to previously described cortical representations. *Somatosens Motor Res.* 13:187–197.
- Xu J, Wall JT. 1997. Rapid changes in brainstem maps of adult primates after peripheral injury. *Brain Res.* 774:211–215.
- Xu J, Wall JT. 1999a. Evidence for brainstem and supra-brainstem contributions to rapid cortical plasticity in adult monkeys. *J Neurosci.* 19:7578–7590.
- Xu J, Wall JT. 1999b. Functional organization of tactile inputs from the hand in the cuneate nucleus and its relationship to organization in the somatosensory cortex. *J Comp Neurol.* 411:369–389.